Chemical Bonding in XeF_2, XeF_4, KrF_2, KrF_4, RnF_2, $XeCl_2$, and $XeBr_2$: From the Gas Phase to the Solid State

Meng-Sheng Liao* and Qian-Er Zhang

State Key Laboratory for Physical Chemistry of Solid Surfaces, Chemistry Department, Xiamen University, Xiamen 361005, P.R. China

Received: June 9, 1998; In Final Form: September 23, 1998

This paper presents a systematic investigation of chemical bonding in a series of noble-gas halides in both the gas phase and the solid state. The crystalline environment was simulated by a cutoff type Madelung potential. Geometries, dissociation energies, force constants, and enthalpies of formation and of sublimation were determined. The calculated properties are in good agreement with available experimental data. The crystal field model is capable of reproducing all significant differences observed between the gas phase and the solid state. KrF_4, $XeCl_2$, and $XeBr_2$ are predicted to be rather unstable against molecular dissociation. The stabilities of the dihalides follow the order $KrF_2 \ll XeF_2 < RnF_2$ and $XeF_2 \gg XeCl_2 \approx XeBr_2$. The calculated trends account for the fact that only the heavier noble gases form compounds and that the electronegativity of the ligand has to be large. The outer polarization orbitals play an important role in the bonding. Relativistic effects on the molecular properties are negligible.

1. Introduction

Since "$XePtF_6$" was prepared in 1962,[1] a number of noble-gas compounds have been synthesized and characterized.[2−4] There is now quite an extensive chemistry of xenon. The most stable xenon compounds are the three colorless fluorides XeF_2, XeF_4, and XeF_6. Since the chemical stability of noble-gas compounds seems to violate the "octet rule", bonding in noble-gas compounds has attracted much attention from both theorists and experimentalists. Various approaches have been proposed. In the past when ab initio calculations were impossible, the bonding and electronic structure of the xenon fluorides were studied using the semiempirical molecular orbital (MO) model as well as the valence bond model. The early semiempirical MO model represents a bonding scheme involving mainly p_σ atomic orbitals. The view can be taken that three-center two-electron σ bonds are involved. In the case of XeF_2, for example, three p_z orbitals combine to form a bonding, a nonbonding, and an antibonding orbital, of which only the first two are occupied, giving a net bond order of 0.5. The simple MO model was widely accepted. However, the disadvantage of any semiempirical model is that no reliable predictions of the bonding energy and of stability can be made. In the valence bond method, Coulson[5] proposed an ionic-valence resonance model for the binding of XeF_2. Indeed, the structures F^-Xe^+F and FXe^+F^- are quite stable, and the ab initio calculations of Bagus et al.[6] support Coulson's picture of the bonding in KrF_2 and XeF_2. In the conventional hybridization model, the structures of XeF_2 and XeF_4 may be described in terms of two-center two-electron bonds as involving the Xe atoms having valence shells containing 10 and 12 electrons, respectively, where the Xe 5s, 5p, and 5d are used to construct sp^3d^n hybrids ($n = 1, 2$). Besides, the electron correlation model was also suggested to account for the qualitative features of the bonding in the noble-gas fluorides.[3] The Hartree−Fock (HF) SCF calculations[6] failed to give a stable XeF_2 molecule, providing support for the electron correlation interpretation. Therefore, on the basis of different theoretical framework, explanations of the bonding in the noble-gas compounds may be given in different manners, which are complementary, rather than contradictory. On the other hand, controversy exists concerning the degree of involvement of "higher" or "outer" orbital of the noble-gas atom in bonding. In particular, the unconventional nature of noble-gas compounds has led some authors to suggest that *n*d and $(n - 1)$f orbitals might in some sense be responsible for the existence of molecules such as XeF_2. However, there have been no extensive studies for this topic.[6,18] So far, the XeF_n ($n = 2, 4, 6$) molecules have been studied by various calculational methods: ab initio,[6−12] Dirac−Slater discrete variational,[13] multiple scattering X_α,[14] relativistic EHMO,[15] and relativistic ab initio all-electron Dirac−Fock−Breit.[16] Theoretical studies of the KrF_2 molecule at the ab initio level were reported by Collins et al.,[17] Bagus et al.,[18] and Bürger et al.[11] Dolg et al.[19] have performed energy-adjusted quasirelativistic pseudo-potential (PP) calculations on RnF_n ($n = 2, 4, 6, 8$). Using a relativistic density functional method, we want to investigate systematically the various noble-gas compounds (XeF_2, XeF_4, KrF_2, KrF_4, RnF_2, $XeCl_2$, $XeBr_2$) and to make predictions of their (unknown) properties. It is known that the xenon fluorides are thermodynamically stable, but the chlorides and the bromides are not. The only experimental information for $XeCl_2$ is the infrared absorption at 313 cm^{-1}.[20] $XeBr_2$ is too unstable to be characterized experimentally. $XeCl_2$ and $XeBr_2$ were obtained only by some special methods.[2,20] KrF_2 is a thermodynamically unstable compound that decomposes spontaneously even at room temperature. The spontaneous dissociation has prevented the accurate determination of a number of the physical properties of KrF_2. There was a claim for the preparation of KrF_4, but this compound has not been well characterized and its structure is unknown. Radon could be combined with fluorine to give a compound of low volatility. The compound was thought to be RnF_2. Because of the short half-life of radon (~3.82 days) and the α-activity of its compounds, it has not been possible to study the compound

* Corresponding author.

10.1021/jp9825516 CCC: $15.00
Published on Web 12/03/1998

in any detail. Since the bond energy of Xe−F in XeF_2 is much larger than that of Kr−F in KrF_2, one expects that the Rn−F bond is at least as energetic as the Xe−F bond. Experimental difficulties make the substance an attractive candidate for theoretical investigations. In this paper, we are concerned not only with the gas-phase free molecules but also with the solid-state compounds. Our investigation focuses on the following properties of the systems: bond length, bond strength (dissociation energy), force constant, vibrational frequency, charge distribution, thermodynamic stability, and relativistic effects. We will discuss effects of *n*d as well as (*n* − 1)f polarization orbitals on the molecular properties. By calculating the various properties, we want to add to our understanding of bonding in the noble-gas compounds.

2. Computational Details

2.1. Density Functional Method. The calculations were carried out by the Amsterdam density functional (ADF) program system developed by Baerends et al.[21] In the ADF method, the molecular orbitals are expanded as linear combinations of Slater-type (STO) basis sets. The specified core electrons are described in the frozen-core approximation. Integrals are computed numerically. Relativistic corrections are calculated by the quasi-relativistic method.[22] Many exchange-correlation potential functionals are included. They are Slater's X_α exchange, Vosko−Wilk−Nusair correlation (VWN),[23] Becke's gradient correction for exchange (B),[24] Perdew−Wang's gradient correction for exchange (PWx),[25,26] Stoll's self-interaction correction for correlation (S),[27] and Perdew's gradient correction for correlation (P).[28] The X_α and VWN functionals are also called the local density approximation (LDA), and the gradient corrections are called the "nonlocal" corrections. These can be combined to give various functionals. It was concluded that the VWN−B−P functional can give accurate bonding energies for both main-group and transition metal systems.[29] But the conclusion may not be true for some particular systems. We found that the VWN−B−P functional (still) greatly overestimates the bonding energies of XeF_2 and F_2 and also gives somewhat too long bond lengths. Therefore we will perform an extensive test of the different density-functionals on XeF_2 and F_2, and then choose the "best" one in the final calculations. Concerning the basis sets, we used a triple-ζ STO basis for the noble-gas *n*s−*n*p valence shells plus two *n*d and one (*n* − 1)f (*n*f in the case of Kr) polarization functions. For the halogen *n*s−*n*p valence shells, a triple-ζ STO basis plus one *n*d ((*n* + 1)d in the case of F) polarization function was employed. Single-ζ STOs are used for core orthogonalization. The shells of lower energy were considered as core and kept frozen.

2.2. Crystal Structures and Solid-State Modeling. The crystal structures of XeF_2 and XeF_4 have been well characterized by the neutron diffraction method.[30,31] XeF_2 is tetragonal with space group *I*4/*mmm*. A unit cell of XeF_2 is shown in Figure 1, and the lattice constants are given in Table 1. The XeF_2 crystalline solid consists of parallel linear XeF_2 units. The Xe atoms are located at the corner and at the body center. Each F atom has one F neighbor at 3.02 Å and four at 3.08 Å. XeF_4 belongs to the monoclinic system and crystallizes in space group $P2_1/n$. The dimensions of the unit cell is given in Table 1. The structure consists of a molecular packing of square-planar molecules of XeF_4. Information about the crystal KrF_2 structure is rather limited. A preliminary X-ray determination[32] indicated that the symmetry of the structure is tetragonal with the lattice constants $a = b = 6.533$ Å and $c = 5.831$ Å, but the space group and bond distances have not been established. It is known

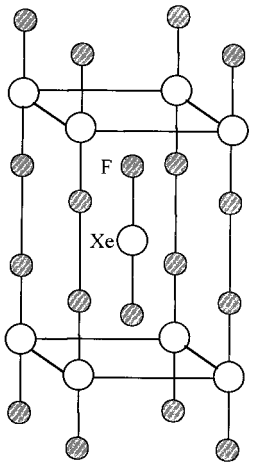

Figure 1. Unit cell of XeF_2.

that crystalline KrF_2 is essentially a molecular assembly. Crystal structures of the solid RnF_2 and $XeCl_2$ compounds have not been characterized experimentally. To explore and predict the properties of the molecules in the solid state, hypothetical crystal compounds were used in the calculations. We assumed the crystal structures of XeF_2 for KrF_2, RnF_2, and $XeCl_2$. However, the lattice constants have to be scaled appropriately. In Figure 1, the nearest interatomic Xe−Xe distance represents the lattice constant *a*. The $\vec{c}$ direction contains two Xe−F entities in a unit cell. We found that the lattice constants of XeF_2 can be determined as

$$a = b \approx 2R_{Xe}^{vdW}; \quad c \approx 2R_{XeF} + 2R_F^{vdW} \tag{1}$$

Here R_{Xe}^{vdW} and R_F^{vdW} are van der Waals (vdW) radii of Xe and F, respectively.[33] We have $2R_{Xe}^{vdW} = 2 \times 2.16 = 4.32$ Å and $2R_{XeF} + 2R_F^{vdW} = 7.00$ Å, which are very close to the lattice constants of $a = 4.315$ and $c = 6.990$ Å, respectively. Therefore, eq 1 has been used to determine the lattice constants of the hypothetical crystal KrF_2, RnF_2, and $XeCl_2$ compounds. The vdW radii of Kr, Rn, and Cl are given to be 2.02, 2.14, and 1.70 Å, respectively.[33] Very recently, Pyykkö[34] provided another set of vdW radii for noble-gas elements: Kr, 2.00 Å; Xe, 2.18 Å; Rn, 2.24 Å. Pyykkö's vdW radius of Rn is 0.1 Å larger than the previously derived value. For Kr and Xe, the two sets of vdW radii are very close. So in the case of Rn, both Bondi's and Pyykkö's radii were adopted and we have two sets of lattice constants (*a*, *b*) for RnF_2. According to the experiments, the Xe−F bond length is about 0.02 Å shorter in the gas phase than in the solid state. For RnF_2 and $XeCl_2$, however, the gas-phase Rn−F and Xe−Cl bond lengths are also unknown experimentally. We therefore used the calculated bond lengths of the free molecules (R^{calc} + 0.02 Å) to approximate R^{exp} in the crystal. Meanwhile, the calculated error in R^{calc} was taken into account. The obtained lattice constants are given in Table 1. To take into consideration the effect of the crystalline environment, the atoms outside the calculated molecule are replaced with point charges. The effects of all point charges are then summed up to convergence by a Madelung-type treatment.[35] The Madelung potential is evaluated on a point grid in the spatial region of the molecular group and is then simulated by fitted charges at a finite number (40−100) of surrounding points of the real crystal lattice. First, the point-charges used for the Madelung potential (MP) calculation is obtained from a Mulliken population analysis of the free molecule. The resulting new charge from the ADF calculation is then fed back into the

TABLE 1: Crystal Structure Data and the Used Bond Lengths[a]

compound	crystal structure data	bond length used
XeF_2	tetragonal, I_4/mmm, $Z = 2$, $a = b = 4.315$, $c = 6.990$	Xe−F = 2.00 (exptl)
XeF_4	monoclinic, $P2_1/c$, $Z = 2$, $a = 5.050$, $b = 5.922$, $c = 5.771$, $\beta = 99.6°$	Xe−F = 1.954 (exptl)
KrF_2 (hypoth)	tetragonal, I_4/mmm, $Z = 2$, Kr−F = 1.90 $a = b = 4.04$, $c = 6.78$	Kr−F = 1.90
RnF_2 (hypoth)	tetragonal, I_4/mmm, $Z = 2$, Rn−F = 2.08 $a = b = 4.28$ (4.48),[b] $c = 7.16$	Rn−F = 2.08
$XeCl_2$ (hypoth)	tetragonal, I_4/mmm, $Z = 2$, Xe−Cl = 2.51 $a = b = 4.315$, $c = 8.42$	Xe−Cl = 2.51

[a] Lattice constants and bond lengths are in angstroms. [b] Determined by Pyykkö's vdW radius of Rn.[34]

MP calculation. The process was repeated with the corrected field until convergence was reached. For comparison, we have also performed a calculation based on a purely ionic picture ($F^--Xe^{2+}-F^-$) for defining the Madelung potential. To further examine the influence of the change of the crystal field on the calculated results, the Mulliken charges of free XeF_2 was also used in the MP approach for test purposes. Because the simple point-charge model neglects the short-range overlap from the nearest neighbors, a slight modification for the Madelung potential has been made by using a Coulomb cutoff-type pseudopotential

$$V_{\text{effective}}(r) = \max(V_{\text{Madelung}}(r), C) \tag{2}$$

It accounts for the fact that the valence electrons of the molecular group must not penetrate into the electrostatically attractive core regions of the surrounding anions or cations because of the Pauli exclusion repulsion. C is a constant used in cutoff-type effective core potentials[36] to balance the nuclear attraction. The bond energy in the crystal field (CF) is defined as AB(in CF) → A(free) + B(free). It now consists of two parts

$$E_{\text{bond}}^{\text{total}} = \frac{1}{2}E_{\text{latt}} + E_{\text{bond}}^{\text{internal}} \tag{3}$$

where $E_{\text{bond}}^{\text{internal}}$ is the bond energy of the molecule, as calculated in the crystal field. E_{latt} is the electrostatic interaction between the fragments and the lattice

$$E_{\text{latt}} = \sum_A [\int \rho_A(\vec{r}) \cdot MP(\vec{r}) \cdot \mathrm{d}\vec{r} + Z_A \cdot MP(R_A)] \tag{4}$$

The cutoff point-charge model has proven to be quite effective in predicting the bonding energies and geometries of isolated molecules or ions in the solid state.[37]

3. Performance of the Density Functionals

Here we give a comparison of the performance of the various functionals in calculating the properties (bond length R_e and dissociation energy D_e) of XeF_2 and F_2. There are experimental data[11,38] that can serve as a means of testing the different functionals. The calculated and experimental data are shown in Table 2. For F_2, the bond length calculated with the VWN−B−P functional agrees well with the experimental value, the error being 0.016 Å. In the case of XeF_2, the VWN−B−P functional gives a bond length that is 0.08 Å too long. All other functionals, when combined with Becke's correction, yield even longer bond lengths than the VWN−B−P one. The effects of "B" and "PW91x" corrections on the calculated results are shown to be similar. Without the gradient corrections for exchange, the calculated dissociation energies are all seriously overestimated. The VWN−B−P values are also too large by more than 1 eV. Among the various functionals, the X_α−B functional gives the smallest dissociation energies, which are 0.45 and 0.4 eV larger than the experimental values for F_2 and XeF_2, respectively. However, the corresponding bond lengths

TABLE 2: Calculated Bond Lengths R_e (Å) and Dissociation Energies D_e (eV) of F_2, XeF_2, Cl_2, and Br_2 with Various Density Functionals[a]

	method	R_e	$R^{\text{calc}}-R^{\text{exp}}$	D_e	$D^{\text{calc}}-D^{\text{exp}}$
F_2	VWN−B−P	1.428	0.016	2.74	1.08
	X_α	1.400	−0.012	3.01	1.35
	X_α−B	1.453	0.041	2.11	0.45
				2.05[b]	
	VWN−S	1.408	−0.004	3.17	1.51
	VWN−S−B	1.463	0.051	2.27	0.61
	VWN−B	1.452	0.040	2.39	0.73
	VWN−PW86x−P	1.447	0.035	2.70	1.04
	VWN−PW92x	1.450	0.038	2.53	0.87
	VWN−PW92x−P	1.427	0.015	2.88	1.22
	exptl[c]	1.412		1.66	
XeF_2	VWN−B−P	2.057	0.079	4.02	1.24
	X_α	2.024	0.046	4.60	1.82
	X_α−B	2.100	0.122	3.16	0.38
	VWN−S	2.036	0.058	4.75	1.97
	VWN−S−B	2.110	0.132	3.31	0.53
	VWN−B	2.094	0.116	3.56	0.78
	exptl	1.978[d]		2.78[e]	
Cl_2	X_α	2.037	0.049	2.95	0.43
	X_α−B	2.108	0.120	1.98	−0.54
				1.94[b]	
	exptl[c]	1.988		2.52	
Br_2	X_α	2.345	0.064	2.43	0.44
	X_α−B	2.430	0.149	1.55	−0.44
				1.51[b]	
	exptl[c]	2.281		1.99	

[a] For the abbreviations, see text. [b] Calculated at the X_α bond length. [c] Reference 38. [d] Reference 11. [e] Reference 2.

are 0.04 and 0.12 Å longer than R^{exp}. The error in R^{calc} is remarkable for XeF_2. It is clear that none of the density functional approximations is adequate for XeF_2. To solve such a problem, some authors[39] suggested a simple, although "inconsistent" procedure. Namely, the bond lengths are optimized at the LDA level, and then Becke's correction is added in a "post-LDA" manner at the optimized LDA bond length. We decide to adopt this procedure in our final calculations in order to obtain relatively accurate results for both bond lengths and dissociation energies. The LDA used here is based on the simple X_α functional. When the X_α and X_α−B functionals are applied to Cl_2, the situations are somewhat different. The D_e calculated with the X_α is only 0.43 eV overestimated, while the X_α−B value is too small by 0.54 eV, i.e., 0.27 eV per Cl. Similar situations are found for Br_2. It is necessary to take the error into account when calculating the D_e's of $XeCl_2$ and $XeBr_2$ by using the "post-LDA" approach.

4. Results and Discussion

The calculated results for the various noble-gas compounds, both in the gas phase and in the solid state, are collected in Tables 3−5, together with available experimental data. For the gas-phase XeF_2, KrF_2, and XeF_4, the molecular properties have been experimentally determined by different authors. The more recent data obtained by Bürger et al.[11,12] from high-resolution infrared studies are believed to be the most accurate. Table 3

TABLE 3: Calculated Properties[a] of the Free Molecules (FM) and the Molecules in the Crystal Fields (MCF)

		R_e	D_e	$\frac{1}{2}E_{latt}$	k_e^s	ω_e^s	k^{as}	ω^{as}
XeF_2	FM	2.024	3.05		2.86	504	2.65	550
	exptl[b]	$1.977_3 \pm 0.0015$	2.78		2.84	515	2.71	558
	exptl[c]	1.977965			2.950	519.2	2.803	560.2
	MCF(A)[d]	2.047	3.99	0.06	2.63			
	MCF(B)[d]	2.036	3.54	0.03	2.75			
	MCF(C)[d]	2.037	3.59	0.04	2.74	493	2.55	540
	exptl[b]	2.00	(3.35)[e]		2.77[f]	496	2.60	547
XeF_4	FM	1.985	5.92		3.28	539		
	exptl[g]	1.94 ± 0.01	5.69		3.3039[h]	550−553		
					3.30[h]			
					3.45[h]			
	exptl[i]	1.93487				554.3		
	MCF	1.996	6.50	0.13	3.12	526		
	exptl[g]	1.954	(6.35)[e]		3.32[f]	543		
KrF_2	FM	1.912	1.69		2.71	490	2.76	596
	exptl[b]	1.875 ± 0.002[j]	1.02		2.46	449	2.66	588
		1.889 ± 0.010[k]						
	exptl[c]	1.88282			2.585	453.2	2.792	592.6
	MCF	1.920	2.11	0.03	2.62	482	2.56	574
	exptl[b]		(∼1.45)[e]		2.41[f]	462	2.59	580
KrF_4	FM	1.886	2.77		2.92	509		
RnF_2	FM	2.103	3.73		2.85	503	2.51	511
	MCF	2.118	4.42	0.06	2.69	489	2.27	486
	MCF[l]	2.116	4.33	0.05	2.70	490	2.29	488
$XeCl_2$	FRM	2.529	0.64		1.40	260	1.33	314
	MCF	2.542	0.96	0.02	1.32	252	1.18	295
	exptl[b]						1.317	313
$XeBr_2$	FM	2.712	0.10		1.08	152	1.09	226

[a] Bond length R_e in angstroms, dissociation energies D_e in eV, symmetrical and antisymmetrical stretching force constants k_e^s and k_e^{as} in N/cm, symmetrical and antisymmetrical stretching vibrational frequencies ω_e^s and ω_e^{as} in cm^{-1}; available experimental data are given for comparison. [b] Reference 2. [c] Reference 11. [d] For the definitions of A, B, and C, see text. [e] Evaluated from D_e(exptl) + ΔH_{sub}(exptl). [f] Evaluated from experimental frequency ω_e using $k = \omega^2 m_F$ (where m_F = mass of F atom). [g] Reference 3. [h] Cited from ref 8. [i] Reference 12. [j] Determined by rotational infrared spectroscopy.[41] [k] Determined by electron diffraction.[42] [l] In the crystal structure with lattice constants *a* and *b* determined by Pyykkö's vdW radius of Rn.

shows that, however, the molecular properties measured by the different authors are in fact quite close. In the earlier rotational infrared studies,[40,41] the Xe−F and Kr−F bond lengths were obtained from the band constant B_0 and these are called the ground-state bond lengths (R_0). Bürger et al. provided both ground-state and equilibrium bond lengths for XeF_2 and KrF_2. The equilibrium bond lengths (R_e) are 0.004−0.006 Å (i.e., <0.01 Å) smaller than the ground-state bond lengths. Bürger et al. did not provide an equilibrium bond length for XeF_4. In some cases,[3,42] the bond lengths were determined by the electron diffraction technique. To be consistent and to compare the different authors' experimental bond lengths, only the ground-state bond lengths are cited by us in the discussion section. Of course, the calculations give only equilibrium bond lengths. There are no direct measurements of the dissociation energy for the crystal compounds. For XeF_2, XeF_4, and KrF_2, experimental enthalpies of sublimation (ΔH_{sub}) are available. The ΔH_{sub} value together with the dissociation energy (D_e^{exp}) of the free molecule can be used to estimate the dissociation energy of the crystal compound, viz. D_e(solid) ≈ ΔH_{sub} + D_e(gas). Similarly, the experimental enthalpy of formation (ΔH_f) of the solid compound may be estimated as $\Delta H_f = nD_e(F_2) - D_e$(solid) ($n$ = 1 or 2). The estimated data are given in parentheses (Tables 3 and 4). By comparison of the calculated energies between the free molecule (FM) and the molecule in crystal field (MCF), we can have the calculational enthalpy of sublimation for the solid compound: ΔH_{sub}(calc) = D_e(MCF) − D_e(FM). The symmetries of free molecule are $D_{\infty h}$ for the dihalides and D_{4h} for the tetrahalides. The gas-phase XeF_2 molecule has been shown to be linear by infrared and Raman spectroscopic experiments.[40] In the crystal field, symmetries of XeF_2 and XeF_4 including the point charges are D_{4h} and C_{2h}, respectively. The calculated bond lengths and force constants were determined from an *n*th degree polynomial fitted to the lowest *m* points ($m > n$).

TABLE 4: Calculated Enthalpies[a] of Formation (ΔH_f) and of Sublimation (ΔH_{sub}) (g = gas, s = solid)

		ΔH_f	ΔH_{sub}
XeF_2 (g)	calcd	−23.1	
	exptl[b]	−25.903[c]	
		−28.2[d]	
		(−25.8)[e]	
XeF_2 (g)	calcd	−35.5	12.5
	exptl[b]	(−39.0)[e]	13.2
			12.3[f]
XeF_4 (g)	calcd	−42.0	
	exptl[g]	−48	
		−51.5	
		(−54.7)[e]	
XeF_4 (s)	calcd	−55.4	13.4
	exptl	(−69.9)[e]	15.3[f]
KrF_2 (g)	calcd	8.3	
	exptl[b]	14.4	
		(14.8)[e]	
KrF_2 (s)	calcd	−1.4	9.7
	exptl[b]	(4.8)[e]	∼9.9
KrF_4 (g)	calcd	30.7	
RnF_2 (g)	calcd	−38.7	
RnF_2 (s)	calcd	−54.7	15.9
	calcd[h]	−52.6	13.8
$XeCl_2$ (g)	calcd	30.0	
$XeCl_2$ (s)	calcd	22.6	7.4
$XeBr_2$ (g)	calcd	32.5	

[a] Enthalpy ΔH in kcal/mol (1 eV = 23.06 kcal/mol); available experimental data are given for comparion. [b] Reference 2. [c] From equilibrium constant data. [d] From calorimetric study. [e] Evaluated from the D_e(exptl) value of F_2 and the D_e(exptl) values given in Table 3. [f] Reference 46. [g] Reference 3. [h] Calculated in the crystal structure with lattice constants *a* and *b* determined by Pyykkö's vdW radius of Rn.

4.1. XeF_2. According to the discussion in section 3, relatively good results can be obtained for XeF_2 by using the "post-LDA"

TABLE 5: Gross Mulliken Populations and Atomic Charges *q* on the Noble Gas and Halogen (FM = Free Molecule; MCF = Molecule in Crystal Field)

		noble gas					halogen		
		*n*s	*n*p	*n*d	$(n-1)$f	q	*n*p	*n*d	q
XeF_2	FM	1.97	4.77	0.18	0.08	1.00	5.48	0.02	−0.50
	MCF	1.97	4.71	0.13	0.07	1.12	5.54	0.02	−0.56
XeF_4	FM	1.89	3.63	0.28	0.21	2.00	5.48	0.02	−0.50
	MCF	1.89	3.59	0.24	0.20	2.08	5.51	0.02	−0.54
KrF_2	FM	1.98	4.93	0.17	0.05	0.86	5.41	0.02	−0.43
	MCF	1.98	4.87	0.13	0.04	0.98	5.47	0.02	−0.49
KrF_4	FM	1.92	4.00	0.23	0.17	1.68	5.40	0.02	−0.42
RnF_2	FM	2.00	4.72	0.14	0.05	1.10	5.52	0.02	−0.55
	MCF	2.00	4.65	0.09	0.04	1.22	5.59	0.02	−0.61
$XeCl_2$	FM	2.00	5.20	0.23	0.05	0.52	5.23	0.03	−0.26
	MCF	2.00	5.11	0.15	0.04	0.70	5.32	0.03	−0.35
$XeBr_2$	FM	2.00	5.31	0.21	0.03	0.44	5.20	0.03	−0.22

approach. For the free molecule, the calculation overestimates the bond length and dissociation energy by 0.046 Å and 0.27 eV, respectively. The errors in both R_e and D_e are small. Especially, the experimental stretching force constants and frequencies for both symmetrical and antisymmetrical modes are very well reproduced by the calculation. From the Mulliken population analysis, F in free XeF_2 bears a net negative charge of −0.5 (see Table 5). So the bonding may be termed "semi-ionic".[3] There also exists some experimental information concerning the charge distribution for the molecule. The atomic charge q_F based on Mössbauer[43] and NMR[44] experiments is rather high (−0.7). In contrast, the atomic charge derived from photoelectron spectroscopy (PES)[45] is small (−0.24). There was no explanation for the large discrepancy.[45] Our calculated value is between the two sets of "experimental" data. Depending on the charge distributions $X^{-q}-Xe^{2q}-X^{-q}$ used, XeF_2 has been treated in three different Madelung potentials. In Table 3, the MCF is labeled A, B, and C with the following meaning: (A) the point charges of −1 (F) and +2 (Xe) are used for defining the MP; (B) the point charges used for the MP are based on Mulliken population analysis of free XeF_2; (C) the charge is maintained with self-consistency, namely, the point charges used for the MP are consistent with the atomic charges of XeF_2 calculated in the crystal field.

Let us first discuss the results of items B and C. From Table 5, we see that the ionicity of the Xe−F bond in the solid is increased by the crystal field, the q_F for MCF being −0.56. The differences Δ between the MCF(B) and MCF(C) values are shown to be very small ($\Delta R = 0.001$ Å, $\Delta D = 0.05$ eV, $\Delta k = 0.01$ N/cm). Therefore the relatively small difference in q used for the MP does not nearly change the calculated results. The bond length calculated in CF(C) is 0.037 Å longer than the crystalline value of 2.00 Å from neutron diffraction. The calculated dissociation energy is 0.24 eV too large. The errors are similar to those obtained for the free molecule. Again, the calculated frequency agrees very well with the experimental value measured in the solid state. From CF(C) to CF(A), the bond length is 0.01 Å lengthened and the dissociation energy is 0.4 eV increased, while the force constant is decreased by 0.1 N/cm. Apparently, the results calculated in CF(A) are less closer to the experimental data than those in CF(C). However, the relatively small changes in R_e, D_e, and k_e also indicate that the calculated results are not sensitive to the change of the crystal field. The calculation also reproduces some subtle details noted in the experimental properties. (1) The bond length is slightly expanded when going from the gas phase to the solid state. (2) Corresponding to the slight Xe−F bond expansion in the CF, there is a slight decrease in the force constant although there exists a CF stabilization effect. The difference Δ = gas-phase value − solid-state value amounts to Δ(exptl) = −0.02 Å for R_{XeF}, to be compared to Δ(calc) = −0.013 Å. For the Xe−F force constant, the values are Δ(exptl) = 0.07−0.18 N/cm and Δ(calc) = 0.12 N/cm. The calculated ΔH_{sub} of 12.5 kcal/mol is in excellent agreement with the experimental values.[2,46] Because the calculated ΔH_{sub} is the difference between D_e(MCF) and D_e(FM), the errors brought about by the density functional used will cancel, i.e., the ΔH_{sub}(calc) would be independent of the density functional used. This demonstrates that the point-charge model is capable of describing accurately the effects of the crystalline environment. Jortner et al.[46] proposed an electrostatic interaction model to account for ΔH_{sub} ($\Delta H_{sub}^{electros} = 45.2 q_F^2$ kcal/mol). By assuming a point charge of −0.5 on each F ligand, they obtained an electrostatic stabilization energy of 11.3 kcal/mol. The dispersion energy and repulsive overlap forces contribute ∼2 kcal/mol to ΔH_{sub}, and the sum of the energetic contributions leads to $\Delta H_{sub} = 13.3$ kcal/mol. So the enthalpy of sublimation of XeF_2 can be interpreted in terms of an electrostatic interaction model. Although the model gives the enthalpy of sublimation that is in good agreement with the experimental value, the agreement with experiment should not be overemphasized. This is because the electrostatic stabilization energy is related to q_F^2. The q_F value obtained by a different method may be rather different. On the other hand, the negative charge on F in the crystal is in fact higher than in the free molecule (−0.6 instead of −0.5 in the free molecule). The enthalpy of sublimation also represents the crystal field stabilization energy on XeF_2. Hence, the crystal field enhances the bonding only mildly. The contribution of the lattice energy (E_{latt}/2) defined in eq 4 is actually very small (<0.1 eV). Let us now discuss the thermodynamic stability of XeF_2. The enthalpy of formation

$$F_2(g) + Xe(g) \rightarrow XeF_2 \qquad (5)$$

is a measure of the thermodynamic stability of the XeF_2 compound. The ΔH_f value can be given by $D_e(F_2) - D_e(XeF_2)$. The enthalpy of the compound will be exothermic if $D_e(XeF_2)$ exceeds $D_e(F_2)$. The calculated $D_e(F_2)$ and $D_e(XeF_2,FM)$ are 0.39 and 0.27 eV too large, respectively. So errors in the calculated ΔH_f partially cancel. According to the calculation, the gaseous XeF_2 is stable with respect to the molecular dissociation by 23 kcal/mol. The different experimental methods give slightly different *standard* enthalpies of formation of the gaseous compound, being 25.9 and 28.2 kcal/mol. The value estimated from the experimental D_e's is 25.8 kcal/mol. All these data are close to the calculated value. The enthalpy of formation of the solid XeF_2 is calculated to be −35.5 kcal/mol, again in good agreement with the estimated value (−39 kcal/mol).

4.2. XeF_4. The calculation on free XeF_4 gives a bond length of 1.985 Å, which is 0.045 Å longer than the experimental value. The Xe−F bond undergoes a contraction upon going from XeF_2 to XeF_4. Xe in XeF_4 bears a charge of +2 (Table 5). So more positive charge on Xe would lead to a contraction in the atomic size. The contraction of 0.04 Å observed experimentally is correctly reproduced by the calculation. Correspondingly, the stretching force constant increases (by 0.4−0.6 N/cm) from XeF_2 to XeF_4. The experimental data of the force constant vary from 3.3 to 3.45 N/cm, which are in good agreement with the calculated value of 3.28 N/cm. Here we have only calculated the symmetrical stretching force constant. The calculated dissociation energy (5.92 eV) differs by 0.23 eV from the experimental value (5.69 eV). The D_e of XeF_4 is nearly twice as large as that of XeF_2. So the average Xe−F bond energies

in XeF_2 and XeF_4 are similar. The most pronounced effect, as shown for the XeF_2 case, is the bond lengthening as well as the force constant reducing from the FM to MCF. Experimentally, R(gas) − R(solid) and k(gas) − k(solid) amount to −0.014 Å and 0.09 N/cm. They are comparable to the calculated values (−0.011 Å and 0.16 N/cm) in magnitude. The calculated dissociation energy for the MCF is 0.15 eV larger than the estimated value. The agreement between theory and "experiment" is good. The crystal field increases the bonding by 0.58 eV (13.4 kcal/mol). The experimental enthalpy of sublimation is 15.3 kcal/mol. Namely, ΔH_{sub}(calc) differs from ΔH_{sub}(exptl) by only 2 kcal/mol. The ligand F in free XeF_4 is negatively charged by 0.5. This value is the same as the calculated value in XeF_2. The F charges derived by Mössbauer, NMR, and PES values are −0.75, −0.55, and −0.24, respectively. The PES values are independent of the number of fluorines, in qualitative agreement with the calculation, although there are quantitative discrepancies. The constancy of charge transfer is also consistent with some of the thermochemical properties of XeF_2 and XeF_4.[46] The Mössbauer charge (q_F) increases, while the NMR charge decreases with increasing Xe coordination. There is now a relatively large discrepancy between the calculated and experimental ΔH_f data. Because ΔH_f(calc) = $2D_e(F_2) - D_e(XeF_4)$, a relatively large error in $D_e(F_2)$ yields a relatively large error in ΔH_f.

4.3. KrF_2 and KrF_4. The calculated Kr−F bond length of free KrF_2 is longer than the experimental value by 0.023−0.037 Å. Different experimental methods[41,42] have given slightly different Kr−F bond lengths. The Kr−F bond length is ca. 0.1 Å shorter than the Xe−F one. The calculated dissociation energy is found to be significantly larger than the experimental value (by 0.67 eV) even though we have adopted the "post-LDA" approach. The calculated force constant is 0.12−0.25 N/cm overestimated. One notable feature here is that the antisymmetrical force constant (k_e^{as}) is larger than the symmetrical one (k_e^s). This is in contrast to the XeF_2 case, where $k_e^{as} < k_e^s$. The calculated trend is consistent with the experimental one. Although $k^{as} = k^s - k_{rr}$, it was observed that in KrF_2 the bond-stretching interaction constant k_{rr} is negative (−0.20 N/cm,[2] −0.207 N/cm[11]) whereas in XeF_2 it is positive (+0.13 N/cm,[2] +0.147 N/cm[11]). The origin of the negative k_{rr} value for KrF_2 was analyzed in a qualitative manner by Coulson.[5] The F charge in free KrF_2 is calculated as −0.43. The lower polarity of the Kr−F bond, relative to the Xe−F bond, can be attributed to the fact that Kr is more electronegative than Xe. The CF increases the F charge by −0.06. Like k_{XeF}, k_{KrF} is weakly decreased by the CF according to the calculation. Experimentally, however, k_{KrF} in the solid state is no longer smaller than that of the gaseous species. Therefore, k_{KrF} in the real crystal structure of KrF_2 would be somewhat different from that in the hypothetical crystal structure. We also find that in the CF, there is $k_e^{as} < k_e^s$. Experimental enthalpy of sublimation of solid KrF_2 is available, ca. 9.9 kcal/mol,[2] which was derived from vapor-pressure measurements. The calculation on the hypothetical crystal structure gives 9.7 kcal/mol for ΔH_{sub}. The two values are in very close agreement. Similar to Xe−F, the Kr−F bond becomes shorter as the oxidation state increases. The average bond energy in KrF_4 (0.7 eV per Kr−F bond) is smaller than that in KrF_2 (0.85 eV per Kr−F bond). This indicates that bond formation for $KrF_2 + 2F \rightarrow KrF_4$ is energetically less favorable than for $Kr + 2F \rightarrow KrF_2$. Free KrF_2 is predicted to be unbound by ca. 8 kcal/mol with respect to the molecular dissociation Kr + F_2. Because of the partial cancellation of the errors in $D_e^{calc}(F_2)$ and $D_e^{calc}(KrF_2)$, there is a reasonable agreement between the calculated and experimental ΔH_f data (exptl − calc = 0.26 eV = 6 kcal/mol). Relative to Kr + $2F_2$, KrF_4 is unstable by 31 kcal/mol. Therefore, little hope can be held for a synthesis of the higher fluoride. The enthalpy of formation of solid KrF_2 is calculated as −1.4 kcal/mol, whereas the experimental data of $D_e(F_2) - D_e(KrF_2) - \Delta H_{sub}$ give it to be +4.8 kcal/mol.

4.4. RnF_2. There are no experimental data for comparison. Only the calculated values (for the gas phase) from the PP-HF and PP-MP2 methods[19] can be compared. Our calculated bond lengths in FM and MCF are 2.103 and 2.118 Å, respectively. Because the calculation may overestimate the bond length by ca. 0.05 Å, the real (unknown) bond lengths in gas-phase and solid-state RnF_2 should be about 2.05 and 2.07 Å, respectively. The PP-HF method gives a bond length of 2.067 Å. We see that R_{RnF} is ca. 0.08 Å longer than R_{XeF}. So the bond lengths show an increase with an increase in the atomic number of the central atom, viz. Kr−F < Xe−F < Rn−F. The symmetrical force constant k_e^s is comparable to that in XeF_2, while the antisymmetrical force constant k_e^{as} is smaller in RnF_2 than in XeF_2. The $k_e^s - k_e^{as}$ value reflects the degree of interaction between the two adjacent bonds. So this interaction is stronger in RnF_2 than in XeF_2. The calculated dissociation energy of 3.73 eV is considerably larger than that of XeF_2. Hence, RnF_2 should be more stable than XeF_2. There is a more substantial charge transfer from Rn to F than from Xe to F, indicating that Rn is less electronegative than Xe. Our Mulliken atomic charge of 1.10 on Rn is similar to the corresponding value (1.12) obtained from the PP-HF method. The CF also increases the F charge. The enthalpy of sublimation is predicted to be 16 kcal/mol. This value is larger than that of XeF_2. The trend is in parallel with the fact that RnF_2 is a less easily sublimated solid than XeF_2. The calculated enthalpies of formation of gas-phase and solid-state RnF_2 are −38.7 and −54.7 kcal/mol, respectively. The ΔH_f value of gas-phase RnF_2 was predicted by the PP-MP2 calculation to be −0.92 eV (−21.2 kcal/mol), which may be too small. We have also performed calculations on RnF_2 in the crystal structure with lattice constants a and b determined by Pyykkö's vdW radius of Rn. It is shown that in the "new" crystal, there are nearly no changes in the bond length and force constants. The dissociation energy (D_e) and the related enthalpies (ΔH_f and ΔH_{sub}) are found to be 0.1 eV smaller. So the calculated results are insensitive to the change of the lattice constants.

4.5. $XeCl_2$ and $XeBr_2$. No other theoretical studies of $XeCl_2$ and $XeBr_2$ have been reported. For the free $XeCl_2$, the calculation gives a bond length of 2.53 Å and a dissociation energy of 0.64 eV. In section 3, we have shown that the calculated dissociation energy of Cl_2 is ca. 0.5 eV too small by using the "post-LDA" approach. Therefore, real dissociation energy of $XeCl_2$ would be ca. 1.1 eV. This value is still much smaller than the D_e value of XeF_2. Thus, chlorine forms a much weaker Xe−X bond than fluorine. Because the calculated bond length is ca. 0.05 Å too large, the real Xe−Cl bond length is predicted to be 2.48 Å. The force constant (symmetrical or antisymmetrical) of $XeCl_2$ is approximately half that of XeF_2. The lower force constant of $XeCl_2$ also reflects the expected weakness of the Xe−Cl bond relative to the Xe−F bond. The gas-phase $XeCl_2$ is unstable by 30 kcal/mol against dissociation into Xe + Cl_2. The larger bond energy of Cl_2 relative to F_2 and the lower bond energy of chlorides relative to fluorides are responsible for the instability of $XeCl_2$. When $XeCl_2$ is embedded in the crystal, the bond length is slightly extended, from 2.529 to 2.542 Å; the force constants are decreased by ∼0.1 N/cm. For the solid-state $XeCl_2$, there is experimental

TABLE 6: Effect of the Polarization Functions on the Calculated Bond Length *R* (Å), Dissociation Energy *D* (eV), and Force Constant *k* (N/cm)

	polarization function	ΔR	ΔD	Δk^s
XeF_2	d	−0.036	0.52	0.42
	f	−0.016	0.14	0.13
XeF_4	d	−0.033	1.15	0.47
	f	−0.021	0.42	0.20
KrF_2	d	−0.050	0.47	0.45
	f	−0.006	0.06	0.06
KrF_4	d	−0.054	1.07	0.57
	f	−0.008	0.17	0.10
RnF_2	d	−0.013	0.37	0.20
	f	−0.024	0.18	0.15
$XeCl_2$	d	−0.067	0.33	0.24
	f	−0.020	0.08	0.07

information for the antisymmetrical Xe−Cl stretching frequency, from which the antisymmetrical force constant k_e^{as} is deduced to be 1.317 N/cm.[20] The calculated k_e^{as} (1.18 N/cm) is found to be in very good agreement with the experimental value. The CF stabilization energy (i.e., ΔH_{sub}) is rather small, only 7.4 kcal/mol. So solid $XeCl_2$ is a weakly bound aggregate and easily sublimates. In view of the calculated q_F values of XeF_2, KrF_2, and RnF_2, we see that the enthalpy of sublimation is relevant to the bond polarity. Small q_X gives a small ΔH_{sub}. This result supports the electrostatic interaction model of Jortner et al.[46] No experimental information is available for $XeBr_2$. From the calculated ΔH_f values, the instability of $XeBr_2$ is not noticeably higher than that of $XeCl_2$. The average Xe−X bond strength decreases by ca. 0.3 eV from the chloride to the bromide. The difference between $XeBr_2$ and $XeCl_2$ is much less pronounced than the difference between $XeCl_2$ and XeF_2. The bond polarity decreases in the sequence $XeF_2 > XeCl_2 > XeBr_2$. This is consistent with the decrease in electronegativity of the ligands F → Br.

4.6. Relative Involvement of Outer *n*d and (*n* − 1)f Orbitals in Bonding. We have performed calculations on the free molecules with and without *n*d as well as (*n* − 1)f basis sets to examine the effects of the polarization orbitals on the bonding. The values of the respective contributions of the *n*d and (*n* − 1)f functions to R_e, D_e, and k_e are given in Table 6. The results show clearly the importance of the polarization effects. However, the effects of polarization may be rather different for different systems. With use of the *n*d polarization functions, the bond length is shortened by 0.01−0.07 Å. The effect on *R* is small for RnF_2 (0.013 Å), and it is large for $XeCl_2$ (0.07 Å). The force constant is increased by 0.2−0.6 N/cm. The addition of the *n*d polarization contributes to 0.4−1.2 eV to the dissociation energy. The *n*d orbital is occupied by 0.2−0.3 electron, showing a significant *n*d orbital participation in the bonding. The effect of (*n* − 1)f polarization is shown to be considerably smaller than that of *n*d polarization. It contributes −0.01 to −0.02 Å to the bond length, 0.1−0.2 N/cm to the force constant, and 0.1−0.4 eV to the dissociation energy. The gross population on the (*n* − 1)f is less than 0.1 for the dihalides; it is 0.2 for the tetrahalides. The general trends are that (1) the polarization orbitals play a more important role in the higher noble-gas oxidation state than in the lower one, and (2) the importance of the *n*d orbital contributions decreases from Kr to Rn, while the opposite is the case for the (*n* − 1)f contributions.

4.7. Relativistic Effects. The relativistic effects on the calculated molecular properties are given in Table 7. All the Δ^{rel} values are shown to be very small, even for the RnF_2 system.

TABLE 7: Relativistic Effects[a] on the Calculated Bond Length *R* (Å), Dissociation Energy *D* (eV), Force Constant *k* (N/cm), and Atomic Charge q_F

	$\Delta^{rel}R$	Δ^{rel}D	$\Delta^{rel}k^s$	$\Delta^{rel}q_F$
XeF_2	0.002	0.01	0.01	0.00
XeF_4	−0.001	0.02	0.03	−0.01
KrF_2	−0.002	0.04	0.01	0.01
KrF_4	−0.003	0.08	0.03	0.01
RnF_2	0.002	0.14	0.07	0.00
$XeCl_2$	−0.004	0.07	0.03	0.00

[a] $\Delta^{rel}A = A^{rel} - A^{nrel}$.

Our results for Δ^{rel} are in agreement with the Dirac−Fock SCF calculations on XeF_2 and XeF_4 by Malli et al.[16]

5. Conclusions

Quasirelativistic density functional calculations have been carried out to investigate the chemical bonding in a series of noble-gas halides XeF_2, XeF_4, KrF_2, KrF_4, RnF_2, $XeCl_2$, and $XeBr_2$ in the gas phase and in the solid state. Our analysis has focused on the various properties of the systems: bond lengths, dissociation energies, force constants, charge distributions, and enthalpies of formation and of sublimation. By use of a "post-LDA" approach, the calculations can yield results that are in good agreement with available experimental data. The influence of the crystal field on the molecular properties can be well reproduced by a cutoff point-charge model. The experimentally observed differences in bond length and force constant between the isolated and the crystalline molecule matched the calculated differences in sign and magnitude. The stability of the compounds is influenced strongly by the nature of both the central atom and the ligand. The ionization potential of the central atom has to be low, and the electronegativity of the ligand has to be large in the formation of noble-gas compounds. This is the reason that so far only the heavier noble gases (Kr, Xe, Rn) can form chemical compounds and that the stable compounds are formed only with the most electronegative elements (F, O). The contributions of outer polarization orbitals to the bonding are significant. However, the relativistic effects on the molecular properties are negligible. The comparative study of the various noble-gas compounds gives valuable insight into understanding their chemical bondings. The calculated results for a number of unknown properties may provide a reference for future work of experiments.

Acknowledgment. The authors thank a referee for drawing their attention to several papers from recent years. This work was supported by the Natural Science Foundation of Fujian Province, P. R. China.

References and Notes

(1) Bartlett, N. *Proc. Chem. Soc.* **1962**, 218.
(2) Bartlett, N.; Sladky, F. O. *Comprehensive Inorganic Chemistry*; Pergamon: Oxford, 1973; Vol. 1, Chapter 6.
(3) Malm, J. G.; Selig, H.; Jortner, J.; Rice, S. A. *Chem. Rev.* **1965**, *65*, 199.
(4) Greenwood, N. N.; Earshaw, A. *Chemistry of the Elements*; Pergamon Press: Oxford, 1984; Chapter 18.
(5) Coulson, C. A. *J. Chem. Phys.* **1966**, *44*, 468.
(6) Bagus, P. S.; Liu, B.; Liskow, D. H.; Schaefer, H. F., III. *J. Am. Chem. Soc.* **1975**, *97*, 7216.
(7) Basch, H.; Moskowitz, J. M.; Hollister, C.; Hankin, D. *J. Chem. Phys.* **1971**, *55*, 1922.
(8) Bartell, L. S.; Rothman, M. J.; Ewig, C. S.; Van Wazer, J. R. *J. Chem. Phys.* **1980**, *73*, 367.
(9) Rothman, M. J.; Bartell, L. S.; Ewig, C. S.; Van Wazer, J. R. *J. Chem. Phys.* **1980**, *73*, 375.

(10) Huzinaga, S.; Klobukowski, M.; Sakai, Y. *J. Phys. Chem.* **1984**, *88*, 4880.
(11) Bürger, H.; Kuna, R.; Ma, S.; Breidung, J.; Thiel, W. *J. Chem. Phys.* **1994**, *101*, 1.
(12) Bürger, H.; Ma, S.; Breidung, J.; Thiel, W. *J. Chem. Phys.* **1996**, *104*, 4945.
(13) Rosen, A.; Ellis, D. E.; Adachi, H.; Averill, F. W. *J. Chem. Phys.* **1976**, *65*, 3629.
(14) Tse, J. S.; Bristow, D. J.; Bancroft, G. M.; Schrobilgen, G. *Inorg. Chem.* **1979**, *18*, 1766.
(15) Pyykkö, P.; Larsson, S. *Chem. Phys.* **1986**, *101*, 355.
(16) (a) Malli, G. L.; Styszynski, J.; Da Silva, A. B. F. *Int. J. Quantum Chem.* **1995**, *55*, 213, (b) Styszynski, J.; Malli, G. L. *Int. J. Quantum Chem.* **1995**, *55*, 227. (c) Styszynski, J.; Cao, X.-P.; Malli, G. L.; Visscher, L. *J. Comput. Chem.* **1997**, *18*, 601.
(17) Collins, G. A. D.; Gruickshank, D. W. J.; Breeze, A. *Chem. Commun.* **1970**, 884.
(18) Bagus, P. S.; Liu, B.; Schaefer, H. F., III. *J. Am. Chem. Soc.* **1972**, *94*, 6635.
(19) Dolg, M.; Küchle, W.; Stoll, H.; Preuss, H.; Schwerdtfeger, P. *Mol. Phys.* **1991**, *74*, 1265.
(20) Nelson, L. Y.; Pimentel, G. C. *Inorg. Chem.* **1967**, *6*, 1758.
(21) ADF program package, version 2.0.1: (a) Baerends, E. J.; Ellis, D. E.; Ros, P. *Chem. Phys.* **1973**, *2*, 41. (b) te Velde, G.; Baerends, E. J. *J. Comput. Phys.* **1992**, *99*, 84.
(22) Ziegler, T.; Tschinke, V.; Baerends, E. J.; Snijders, J. G.; Ravenek, W. *J. Phys. Chem.* **1989**, *93*, 3050.
(23) Vosko, S. H.; Wilk, L.; Nusair, M. *Can. J. Phys.* **1980**, *58*, 1200.
(24) Becke, A. D. *Phys. Rev.* **1988**, *A38*, 3098.
(25) Perdew, J. P.; Wang, Y. *Phys. Rev.* **1986**, *B33*, 8800.
(26) Perdew, J. P.; Wang, Y. *Phys. Rev.* **1992**, *B46*, 6671.
(27) Stoll, H.; Pavlidou, C. M. E.; Preuss, H. *Theor. Chim. Acta* **1978**, *49*, 143.
(28) Perdew, J. P. *Phys. Rev.* **1986**, *B33*, 8822.
(29) (a) Johnson, B. G.; Gill, P. M. W.; Pople, J. A. *J. Chem. Phys.* **1993**, *98*, 5612. (b) Li, J.; Schreckenbach, G.; Ziegler, T. *J. Am. Chem. Soc.* **1995**, *117*, 486. (c) Heinemann, C.; Hertwig, R. H.; Wesendrup, R.; Koch, W.; Schwarz, H. *J. Am. Chem. Soc.* **1995**, *117*, 495.
(30) Levy, H. A.; Agron, P. A. *J. Am. Chem. Soc.* **1963**, *85*, 241.
(31) (a) Burns, J. H.; Agron, P. A.; Levy, H. A. *Science* **1963**, *139*, 1208. (b) Templeton, D. H.; Zalkin, A.; Forrester, J. D.; Williamson, S. M. *J. Am. Chem. Soc.* **1963**, *85*, 242.
(32) Siegel, S.; Gebert, E. *J. Am. Chem. Soc.* **1964**, *86*, 3896.
(33) Bondi, A. *J. Phys. Chem.* **1964**, *68*, 441
(34) Pyykkö, P. *Chem. Rev.* **1997**, *97*, 597.
(35) Ewald, P. P. *Ann. Phys.* **1921**, *64*, 253.
(36) Kutzelnigg, W.; Koch, R. J.; Bingel, W. A. *Chem. Phys. Lett.* **1968**, *2*, 197.
(37) (a) Liao, M.-S.; Zhang, Q.-E.; Schwarz, W. H. E. *Inorg. Chem.* **1995**, *34*, 5597. (b) Liao, M.-S.; Schwarz, W. H. E. *J. Alloys Compd.* **1997**, *246*, 2.
(38) Huber, K. P.; Herzberg, G. *Molecular Spectra and Molecular Structure, Vol. IV, Constants of Diatomic Molecules*; Van Nostrand Reinhold: New York, 1979.
(39) (a) Ziegler, T.; Tschinke, V.; Becke, A. D. *Polyhedron*, **1987**, *6*, 685. (b) Becke, A. D. *J. Chem. Phys.* **1992**, *96*, 2155.
(40) Reichman, S.; Schreiner, F. *J. Chem. Phys.* **1969**, *51*, 2355.
(41) Murchison, C.; Reichman, S.; Anderson, D.; Overend, J.; Schreiner, F. *J. Am. Chem. Soc.* **1968**, *90*, 5690.
(42) Harshbarger, H.; Bohn, R. K.; Bauer, S. H. *J. Am. Chem. Soc.* **1967**, *89*, 6466.
(43) Perlow, G. J. In *Chemical Application of Mössbauer Spectroscopy*; Goldanskii, V. I., Herber, R. H., Eds.; Academic Press: New York, 1968; p 367.
(44) Hindman, J. C.; Svirmickas, A. In *Noble Gas Compounds*; Hyman, H. H., Ed.; University of Chicago Press: Chicago, IL, 1963; p 251.
(45) Carroll, T. X.; Shaw, R. W.; Thomas, T. D.; Kindle, C.; Bartlett, N. *J. Am. Chem. Soc.* **1974**, *96*, 1989.
(46) Jortner, J.; Wilson, E. G.; Rice, S. A. *J. Am. Chem. Soc.* **1963**, *85*, 814.